ISSN 1070-3284, Russian Journal of Coordination Chemistry, 2023, Vol. 49, No. 12, pp. 771–776. © Pleiades Publishing, Ltd., 2023.
Russian Text © The Author(s), 2023, published in Koordinatsionnaya Khimiya, 2023, Vol. 49, No. 12, pp. 731–736.

Cadmium(II)-Organic Coordination Polymer Containing Carboxyl Groups: Solvothermal Synthesis, Structure, and Properties

B. Xu[a], **W. Yao**[a], **X. Yu**[b, c], **D. G. Samsonenko**[b], **V. P. Fedin**[b, c, *], **and E. Gao**[a, *]

[a] *China-Russian Institute of Engineering Materials Chemistry, School of Chemical Engineering,*
University of Science and Technology Liaoning, Anshan, 114051 China
[b] *Nikolaev Institute of Inorganic Chemistry, Siberian Branch, Russian Academy of Sciences, Novosibirsk, Russia*
[c] *Novosibirsk State University, Novosibirsk, Russia*
**e-mail: cluster@niic.nsc.ru*

Received February 14, 2023; revised February 27, 2023; accepted March 13, 2023

Abstract—New metal-organic coordination polymer Cd[H_2L] (**I**) (where H_4L is 4,4'-([2,2'-bipyridine]-6,6'-diylbis(oxy))diphthalic acid) is synthesized in a high yield under the solvothermal synthesis conditions. According to the X-ray diffraction (XRD) data, each Cd(II) cation binds four organic ligands: one ligand is bound via the coordination of the chelate bipyridyl fragment, two ligands are linked via the bidentate coordination of the deprotonated COO groups, and one ligand is bound via the monodentate coordination of the protonated carboxylate group. The synthesized three-dimensional metal-organic framework contains no free space capable of including guest molecules. Compound **I** is characterized by powder XRD, IR spectroscopy, and elemental (C, H, N) and thermogravimetric analyses. The luminescence spectra of compound **I** are recorded.

Keywords: metal-organic coordination polymers, XRD, polycarboxylate ligands, cadmium(II) complexes, luminescence

DOI: 10.1134/S1070328423600316

INTRODUCTION

Increasing interest in metal-organic coordination polymers (or metal-organic frameworks (MOF)) is primarily due to prospects of their use for the development of functional materials with unique or improved characteristics, which makes it possible to produce, for instance, a new generation of membranes and sensors, heterogeneous catalysts, and proton-conducting materials [1, 2]. Evidently, the properties of MOF are predetermined by the topology of the framework and the nature of inorganic and organic building blocks. The typical examples of polytopic ligands for the preparation of MOF are anions of polycarboxylic acids, and terephthalate is the most widely abundant ligand in the chemistry of these compounds.

Special attention is recently given to the functionalized MOF containing such functional groups as –COOH, –SO_3H, –NH_2, and –SH in the organic fragment [3]. These frameworks can be prepared by direct synthesis or using the post-synthetic modification of the already formed framework. The metal-organic coordination polymers containing free carboxylate groups (MOF-COOH) demonstrate considerable progress and prospects in such applications as adsorption, catalysis, proton conductivity, and sensors [4–7].

The synthesis, structure, and properties of the new MOF Cd[H_2L] built of Cd(II) and 4,4'-([2,2'-bipyridine]-6,6'-diylbis(oxy))diphthalic acid (H_4L) dianions are described in this work. The formed three-dimensional framework contains free carboxyl groups and is thermally and hydrolytically stable but is not porous. The structural formula of H_4L is shown in Scheme 1.

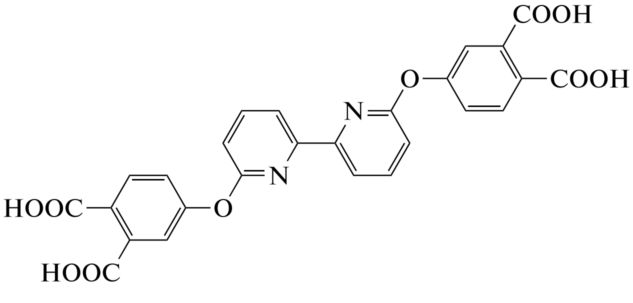

Scheme 1.

EXPERIMENTAL

The purity of all reagents and solvents was not lower than reagent grade, and they were used as received. Ligand H_4L ($C_{26}H_{16}N_2O_{10}$) was presented by Jinan Henghua Sci. & Tec. Co. Ltd.

IR spectra were recorded on a Bruker Scimitar FTS 2000 FT-IR spectrometer in KBr pellets in a range of 4000–400 cm^{-1}. Elemental analysis was carried out on a Vario MICRO cube CHNS analyzer. Powder XRD data were obtained on a Bruker D8 ADVANCE powder diffractometer (CuK_α radiation, λ = 1.54056 Å). Thermogravimetric (TG) analysis was conducted on a NETZSCH TG 209 F1 Iris thermoanalyzer on linear heating samples in a temperature range of 30–850°C at a rate of 10°C/min in a He atmosphere. Solid-state luminescence spectra were recorded on a Horiba Jobin Yvon Fluorolog 3 spectrometer equipped with a 450-W Xe lamp and a PM-1073 PMT detector. Electrical conductivity was measured by electrochemical impedance spectroscopy in a two-electrode cell on a Precision LCR Meter IPU-1RLC-1/2008 instrument in an ac frequency range of 1–3.3 MHz and on an Instek instrument (frequency range 12 Hz–200 kHz). The electrical conductivity at 300°C was measured in an argon atmosphere. The electrical conductivity (σ) was calculated by the following equation: $\sigma = lR^{-1}S^{-1}$, where l is the thickness, R is the electrolyte resistance, and S is the effective surface area of the electrolyte.

Synthesis of cadmium(II) 4,4'-([2,2'-bipyridine]-6,6'-diylbis(oxy))diphthalate Cd[H₂L] (I). A mixture of $Cd(NO_3)_2 \cdot 4H_2O$ (30.8 mg, 0.1 mmol), H_4L (51.6 mg, 0.1 mmol), and an acetonitrile–water (1 : 3, vol/vol) mixture (20 mL) was treated in an ultrasonic bath for 10 min. The resulting mixture was transferred to a 30-mL glass tube, which was sealed and hold at 120°C for 96 h until platy yellow crystals formed. After cooling to room temperature, the crystals were filtered off, washed with an acetonitrile–water (1 : 3, vol/vol) mixture, and dried in air. The yield of compound **I** was 73%.

IR, (KBr; ν, cm^{-1}): 3082 ν(C–H), 1748 ν(COOH), 1718 ν(COOH), 1583 ν_{as}(C=O), 1541 ν_{as}(C=O), 1438 ν_{as}(COO^-), 1143, 1012.

For $C_{26}H_{14}N_2O_{10}Cd$

Anal. calcd., %	C, 49.82	H, 2.25	N, 4.47
Found, %	C, 49.51	H, 2.22	N, 4.61

XRD for a twinned crystal of compound **I** was carried out at 150 K on a Bruker D8 Venture automated diffractometer equipped with an area PHOTON III detector and a microfocus X-ray source (λ(MoK_α) = 0.71073 Å). An absorption correction was applied using the SADABS program [8]. The structure was solved using the SHELXT program [9] and refined by full-matrix least squares in the anisotropic approximation (except for hydrogen atoms) using the SHELXL program [10]. The positions of hydrogen atoms were calculated geometrically and refined by the riding model. The crystallographic data and XRD experimental details are given in Table 1.

The full tables of interatomic distances and bond angles, coordinates of atoms, and atomic displacement parameters were deposited with the Cambridge Crystallographic Data Centre (CIF file CCDC no. 2241352; https://www.ccdc.cam.ac.uk/structures/).

RESULTS AND DISCUSSION

Acid H_4L contains four carboxyl groups (Scheme 1) that can coordinate metal cations and form molecular complexes or coordination polymers. In addition, the ligand bears the bipyridyl fragment that can bind transition metal atoms and ether groups providing a conformational lability of the ligand. Such an interesting, in our opinion, ligand is commercially available, but published data on any its molecular complexes or MOF are lacking.

Platy yellow crystals of compound **I** were obtained in a high yield under solvothermal synthesis conditions on heating stoichiometric amounts of cadmium(II) nitrate and acid H_4L in an acetonitrile–water mixture. When the experimental conditions (reagent ratio, temperature, solvent, synthesis time) are changed, compound **I** is not formed or its yield decreases.

The structure of compound **I** was determined by XRD. According to the XRD data, the asymmetric unit of the structure of compound **I** contains the cadmium(II) cation and H_2L^{2-} dianion. The coordination environment of Cd(II) consists of two nitrogen atoms of the bipyridyl fragment and five oxygen atoms of three COO groups, two of which are coordinated via the bidentate mode (O(1), O(2) and O(9), O(10)) and one group is monodentate-coordinated (O(7)). The bidentate-bound COO groups are coordinated asymmetrically, which appears as the formation of two short (O(1) and O(10)) and two elongated (O(2) and O(9)) Cd–O bonds (Fig. 1). The short Cd–O distances are 2.296(4) and 2.206(3) Å, and the elongated Cd–O distances are 2.732(4) and 2.768(4) Å. The Cd–O distance for the COO group coordinated via the monodentate mode is 2.447(3) Å. The Cd–N distances are 2.298(3) and 2.302(4) Å. Thus, the coordination number of Cd(II) can be described as 5 + 2. According to the data of calculations in the SHAPE program [11], the coordination polyhedron of the cadmium(II) cation is described best of all as a distorted one-capped octahedron (COC-7). The organic ligand contains four carboxylate groups, two of which are protonated (O(3) and O(8)) to form the H_2L^{2-} dianion and two intramolecular hydrogen bonds between the protonated and deprotonated carboxylate groups (Fig. 1). The O...O distances are 2.458(5) and 2.454(6) Å. The Cd(II) cations are bound by the organic dianions into zigzag polymer chains parallel to

Table 1. Crystallographic data and structure refinement parameters for compound **I**

Parameter	Value
Empirical formula	$C_{26}H_{14}N_2O_{10}Cd$
FW	626.79
Crystal system	Monoclinic
Space group	$P2_1/c$
a, Å	14.3665(9)
b, Å	17.9515(12)
c, Å	8.6639(6)
β, deg	93.248(2)
V, Å^3	2230.8(3)
Z	4
ρ_{calc}, g/cm^3	1.866
μ, mm^{-1}	1.049
F(000)	1248
Crystal size, mm	0.14 × 0.13 × 0.03
Scan range over θ, deg	2.61–27.48
Range of indices *hkl*	$0 \le h \le 18$, $-23 \le k \le 0$, $-11 \le l \le 11$
N_{hkl} of measured/independent reflections	56796/5141
R_{int}	0.0638
N_{hkl} with $I > 2\sigma(I)$	4777
GOOF for F^2	1.199
R indices ($I > 2\sigma(I)$)	$R_1 = 0.0329$, $wR_2 = 0.0750$
R indices (for all reflections)	$R_1 = 0.0434$, $wR_2 = 0.0791$
Residual electron density (max/min), e/Å^3	0.547/–0.708

the crystallographic *a* axis. Only the nitrogen atoms (N(1) and N(2)) of the bipyridyl fragment and deprotonated COO groups (O(1), O(2) and O(9), O(10) are involved in the binding. The polymer chains are linked with each other via the coordination of the oxygen atom (O(7)) of one of the protonated carboxylate groups in one chain to the Cd(II) cation of the adjacent chain to form the metal-organic framework (Fig. 2). The topological representation of the metal-organic framework is shown in Fig. 3. The polymer chains alternate along the crystallographic *b* and *c* axes in the chess order, and each chain is linked with four adjacent chains along the *b* axis. Each organic ligand binds four Cd(II) cations via the nitrogen atoms of the bipyridyl fragment and the oxygen atoms of three of four carboxylate groups (two deprotonated groups and one protonated group). One protonated carboxylate group remains uninvolved in the coordination. Each Cd(II) cation binds four organic ligands: one cation coordinates the chelate bipyridyl fragment, two cations coordinate the deprotonated COO groups via the bidentate mode, and one more cation binds the ligand via the monodentate coordination of the protonated carboxylate group. The formed metal-organic framework contains no free space capable of including guest molecules.

Compound **I** was characterized by powder XRD, IR spectroscopy, and TG and elemental analyses. The powder XRD pattern of compound **I** corresponds completely to the pattern calculated from the single-crystal XRD data (Fig. 4). Moreover, the compound showed a high hydrolytic stability and retains its structure on storage in water for 24 h. A high thermal stability of compound **I** was proved by the TG data. No change in the sample weight occurred on heating to 320°C. A significant decrease in the sample weight due to the decomposition of the organic ligand is observed at a higher temperature.

The photophysical properties of complex **I** and ligand H_4L were studied. The excitation spectrum of tetracarboxylic acid exhibits the broad bands with maxima at 340, 380, and 410 nm, and the emission spectrum of the acid sample demonstrates blue emission with a broad band maximum at 482 nm (Fig. 5). The Cd(II) complexes with the electronic configuration d^{10} are not redox-active, and the metal-to-ligand charge transfer (MLCT) or ligand-to-metal charge

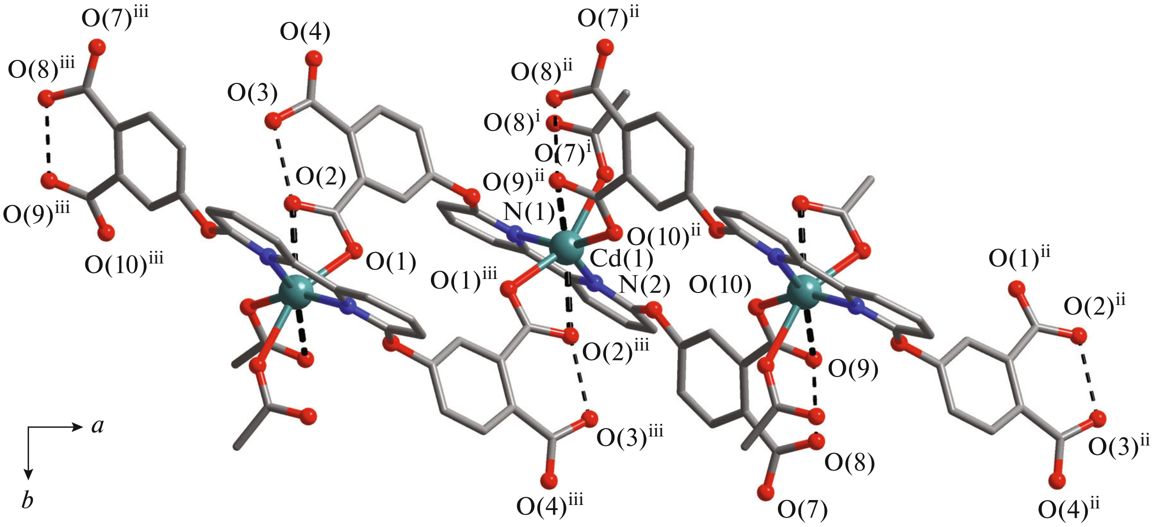

Fig. 1. Fragment of the chain in the structure of compound **I** (hydrogen atoms are omitted). The elongated Cd–O bonds are shown by thick dashed lines, and hydrogen bonds are shown by thin dash. The positions of the related atoms were revealed by the following symmetry operations: (i) $2 - x, y - 1/2, 3/2 - z$; (ii) $2 - x, 1 - y, 1 - z$; (iii) $1 - x, 1 - y, 1 - z$.

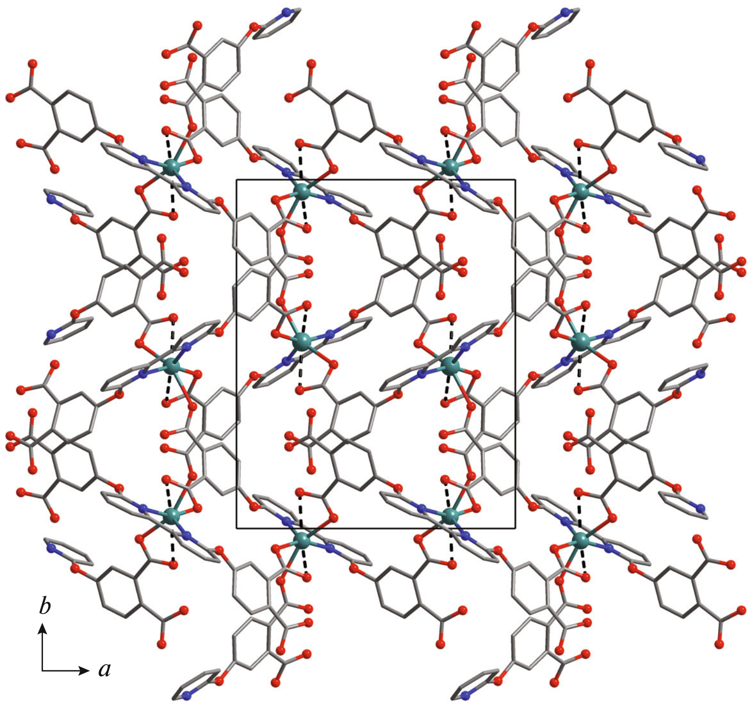

Fig. 2. Fragment of the metal-organic framework in the structure of compound **I** (projection onto the *ab* plane; hydrogen atoms are omitted). The positions of the metal atoms are shown by large balls. The elongated Cd–O bonds are shown by dashed lines.

transfer (LMCT) mechanism is observed. In our case, ligand-centered luminescence occurs for MOF **I**, and the observed emission with the band maximum at 486 nm can be assigned to intraligand transitions $\pi^* \rightarrow \pi$ and/or $\pi^* \rightarrow n$ in the organic ligand. The luminescence decay of MOF **I** obeys a biexponential law with lifetimes of the excited state of 1.72 and 5.33 ns. The short lifetimes in the excited state confirm that the luminescence of the framework is ligand-centered fluorescence.

The MOF-COOH can be potential materials for proton conductivity. Interesting features of compound **I** are the high thermal stability, the presence of protonated carboxylate groups, and the absence of

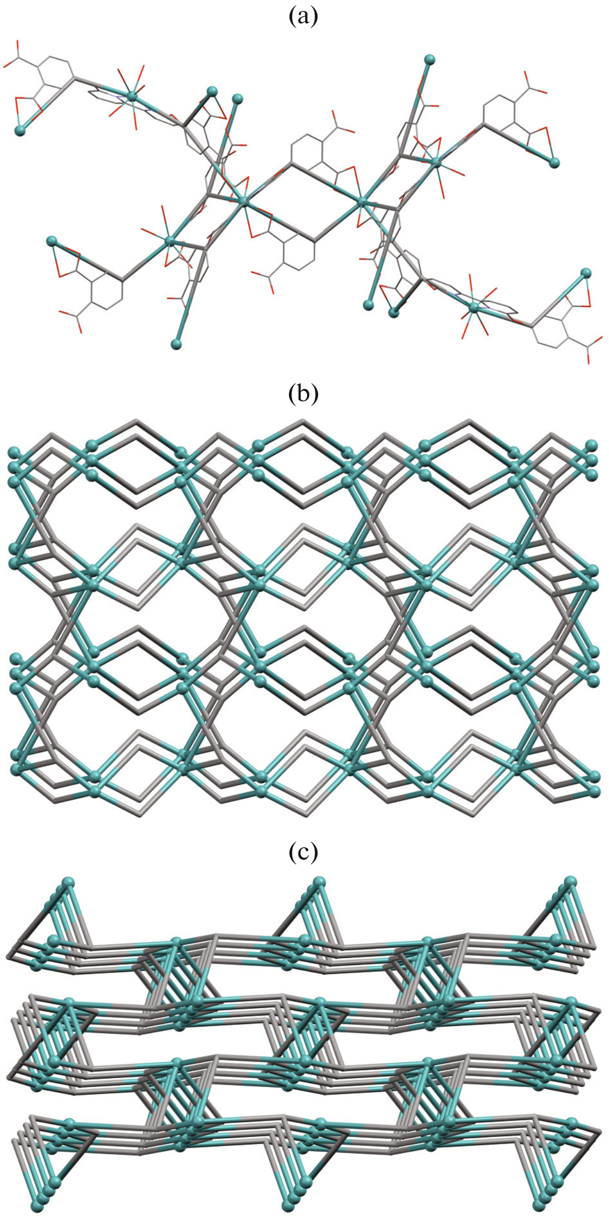

Fig. 3. Representation of the topology of the metal-organic framework in the structure of compound **I**: (a) choice of nodes and edges of the topological network, (b) view along the crystallographic *c* axis, and (c) view along the crystallographic *a* axis. The positions of the metal atoms are shown by balls.

porosity. In principle, proton conductivity is possible at elevated temperature, since COOH groups can be proton sources. Samples of compound **I** were pressed at room temperature and using hot pressing at 150°C. The conductivity was measured in both air and an inert argon atmosphere. The samples were heated to 300°C and hold at this temperature for about 60 min. Unfortunately, the conductivity of the sample at 300°C turned out to be low and did not exceed 10^{-7} S/cm.

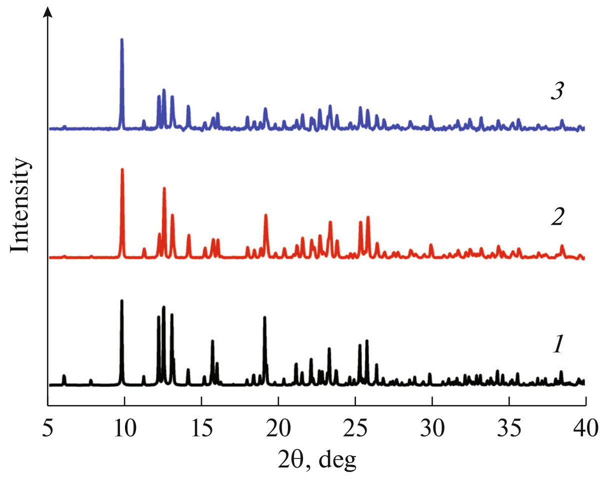

Fig. 4. Powder XRD patterns of compound **I**: (*1*) simulated from the single-crystal XRD data and experimental patterns (*2*) for the sample after the synthesis and (*3*) for the sample stored in water for 24 h.

Porous framework structures with free COOH groups are considered as promising for the development of materials with superprotonic conductivity. However, pores of the known MOF-COOH [12–16] are filled with water molecules, which are proton carriers already at relatively low temperatures. Thus, further studies aimed at synthesizing compounds with superprotonic conductivity will be focused on the synthesis of new hydrolytically stable and porous MOF based on H_4L.

Thus, the new metal-organic coordination polymer Cd[H_2L] (**I**) (H_4L is 4,4'-([2,2'-bipyridine]-6,6'-diylbis(oxy))diphthalic acid) was synthesized in the high yield under the solvothermal synthesis conditions. This is the first example of the coordination compound based on this tetracarboxylate ligand. The

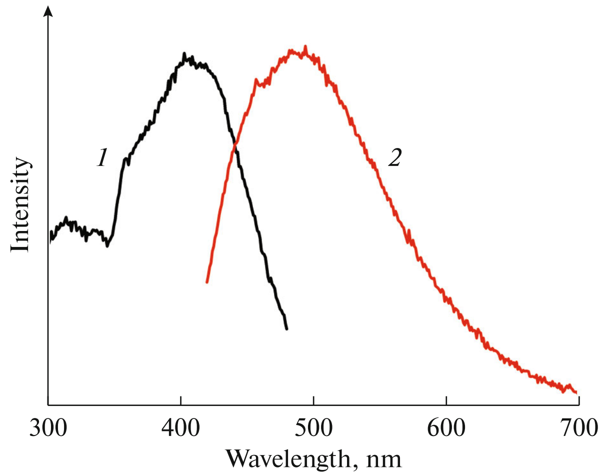

Fig. 5. (*1*) Solid-state excitation and (*2*) solid-state emission spectra of compound **I**.

synthesized 3D metal-organic framework contains no free space capable of including guest molecules and demonstrates high hydrolytic and thermal stabilities and ligand-centered fluorescence.

ACKNOWLEDGMENTS

The authors thank V.G. Ponomareva (Institute of Solid State Chemistry and Mechanochemistry, Siberian Branch, Russian Academy of Sciences).

FUNDING

The analytical characterization of the synthesized compounds was supported by the Ministry of Science and Higher Education of the Russian Federation (project no. 121031700321-3). B. Xu and X. Yu are grateful to the China Scholarship Council (CSC) for financial support (grants nos. 202110340003 and 202008090088).

CONFLICT OF INTEREST

The authors of this work declare that they have no conflicts of interest.

REFERENCES

1. Agafonov, M.A., Alexandrov, E.V., Artyukhova, N.A., et al., *J. Struct. Chem.*, 2022, vol. 63, p. 671.
2. Kirchon, A., Feng, L., Drake, H.F., et al., *Chem. Soc. Rev.*, 2018, vol. 47, p. 8611.
3. Bhadra, B.N., Ahmed, I., Lee, H.J., and Jhung, S.H., *Coord. Chem. Rev.*, 2022, vol. 450, 214237.
4. Yin, H.Q. and Yin, X.B., *Acc. Chem. Res.*, 2020, vol. 53, p. 485.
5. Ji, Z., Wang, H., Canossa, S., et al., *Adv. Funct. Mater.*, 2020, vol. 30, 2000238.
6. Mandal, S., Natarajan, S., Mani, P., and Pankajakshan, A., *Adv. Funct. Mater.*, 2021, vol. 31, 2006291.
7. Razavi, S.A.A. and Morsali, A., *Coord. Chem. Rev.*, 2019, vol. 399, 213023.
8. *Bruker Apex3 Software Suite: Apex3, SADABS-2016/2 and SAINT. Version 2018.7-2*, Madison: Bruker AXS Inc., 2017.
9. Sheldrick, G.M., *Acta Crystallogr., Sect. A: Found. Adv.*, 2015, vol. 71, no. 1, p. 3.
10. Sheldrick, G.M., *Acta Crystallogr., Sect C: Struct. Chem.*, 2015, vol. 71, no. 1, p. 3.
11. Llunell, M., Casanova, D., Cirera, J., et al., *SHAPE. Version 2.1. Program for the Stereochemical Analysis of Molecular Fragments by Means of Continuous Shape Measures and Associated Tools*, Barcelona: Universitat de Barcelona, 2013.
12. Shigematsu, A., Yamada, T., and Kitagawa, H., *J. Am. Chem. Soc.*, 2011, vol. 133, p. 2034.
13. He, T., Zhang, Y.Z., Wu, H., et al., *ChemPhysChem*, 2017, vol. 18, p. 3245.
14. Sun, Z., Yu, S., Zhao, L., et al., *Chem.-Eur. J.*, 2018, vol. 24, no. 42, p. 10829.
15. Qin, Y., Xue, M.-H., Dou, B.-H., et al., *New J. Chem.*, 2020, vol. 44, p. 2741.
16. Su, J., He, W., Li, X.-M., et al., *Matter*, 2020, vol. 2, p. 711.

Translated by E. Yablonskaya